Universality class of replica symmetry breaking, scaling behavior, and the low-temperature fixed-point order function of the Sherrington-Kirkpatrick model

R. Oppermann and M. J. Schmidt
Institut für Theoretische Physik, Universität Würzburg, Am Hubland, 97074 Würzburg, Federal Republic of Germany
(Received 22 April 2008; published 23 December 2008)

A scaling theory of replica symmetry breaking (RSB) in the Sherrington-Kirkpatrick (SK) model is presented in the framework of critical phenomena for the scaling regime of large RSB orders κ, small temperatures T, and small (homogeneous) magnetic fields H. We employ the pseudodynamical picture [R. Oppermann, M. J. Schmidt, and D. Sherrington, Phys. Rev. Lett. **98**, 127201 (2007)], where two critical points $\mathcal{CP}1$ and $\mathcal{CP}2$ are associated with the order function's pseudodynamical limits $\lim_{a\to\infty} q(a)=1$ and $\lim_{a\to 0} q(a)=0$ at $(T=0, H=0, 1/\kappa=0)$. $\mathcal{CP}1$- and $\mathcal{CP}2$-dominated contributions to the free energy functional $F[q(a)]$ require an unconventional scaling hypothesis. We determine the scaling contributions in accordance with detailed numerical self-consistent solutions for up to 200 orders of RSB. Power laws, scaling functions, and crossover lines are obtained. $\mathcal{CP}1$-dominated behavior is found for the nonequilibrium susceptibility, which decays like $\chi_1 = \kappa^{-5/3} f_1(T/\kappa^{-5/3})$, for the entropy, which obeys $S(T=0)\sim\chi_1^2$, and for the subclass of diverging parameters $a_i = \kappa^{5/3} f_{a_i}(T/\kappa^{-5/3})$ [describing Parisi box sizes $m_i(T)\equiv a_i(T)T$], with $f_1(\zeta)\sim\zeta$ and $f_{a_i}(\zeta)\sim 1/\zeta$ for $\zeta\to\infty$, while $f(0)$ is finite. $\mathcal{CP}2$-dominated behavior, controlled by the magnetic field H while temperature is irrelevant, is retrieved in the plateau height (or width) of the order function $q(a)$ according to $q_{pl}(H) = \kappa^{-1} f_{pl}(H^{2/3}/\kappa^{-1})$ with $f_{pl}(\zeta)|_{\zeta\to\infty}\sim\zeta$ and $f_{pl}(0)$ finite. Divergent characteristic RSB orders $\kappa_{\mathcal{CP}1}(T)\sim T^{-3/5}$ and $\kappa_{\mathcal{CP}2}(H)\sim H^{-2/3}$, respectively, describe the crossover from mean field SK- to RSB-critical behavior with rational-valued exponents extracted with high precision from our RSB data. The order function $q(a)$ is obtained as a fixed-point function $q^*(a^*)$ of RSB flow, in agreement with integrated fixed-point energy and susceptibility distributions.

DOI: 10.1103/PhysRevE.78.061124 PACS number(s): 75.10.Nr, 75.40.−s, 89.75.Da

I. INTRODUCTION

The far-reaching usefulness of spin-glass theories [1–3] and of its key structural elements such as frustration, disorder, hierarchical order, ultrametricity, complexity, and freezing transition, is evidenced by applications entering even life sciences and transdisciplinary research fields. Physical models, where these key structures acquired a specific mathematical meaning, find very broad applications beyond their origin in frustrated magnetism. Let us mention, apart from fields like neural networks, computer science, and econophysics, the fascinating sociological applications to opinion and group dynamics [4,5], biological applications to RNA folding [6–8] including the quantum chromodynamical analogy and random matrix theory [9]. For these reasons it seems natural to search for universal features of unifying models both in the general sense and in the precise meaning of the renormalization group [7].

The 3SAT optimization problem [10,11] and its close relation to the $T=0$ Sherrington-Kirkpatrick model [12] or RNA folding in biophysics [6], where glass transitions exist within the secondary RNA structure [7,13,14], provide examples where even the zero temperature limit is either exactly realized or close to the realistic situation. In physics, spin-glass phases are usually confined to a low-temperature regime and some applications are rather remote from it. Yet knowing the ground-state structure remains important. For one of the most fruitful standard models, the Sherrington-Kirkpatrick model [12] (SK model), the hierarchical ground-state structure, as predicted by Parisi three decades ago [15,16], has been confirmed [17]. Yet further explicit analytic solutions and meaningful approximations are still required to improve understanding and to support progress in more complicated (non-mean-field finite-range, or quantum) models.

The attempt to link the SK-model behavior deep inside its ordered (spin-glass) phase to the theory of critical phenomena may appear unmotivated at first sight, since the infinite-ranged spin interaction suggests "only" mean-field behavior. However the SK-model solution is not simple below its thermal mean-field transition. The source of complication is known to be the Parisi replica symmetry breaking (RSB). RSB involves a treelike hierarchical structure of the order parameter [3]. The tree height is cut off [18] in case of a finite RSB order κ. As κ grows to infinity, a characteristic RSB order $\kappa_c(T)$ or tree height can be identified [see, for example, Eqs. (15) and (21) in Sec. IV below], which scales with temperature like $T^{-3/5}$ and hence diverges as $T\to 0$. At high tree levels, hence near the diagonal of the Parisi matrix [3,18], nonlinear effects turn out to be responsible for nonanalytic behavior as a function of the quasicontinuous variable $1/\kappa$. The nonanalytic power laws specify an RSB-universality class, which should be compared with similar behavior in different physical systems and in other scientific fields such as biology, sociology, and (mathematical) psychology, where evidently frustrated random (and in some cases range-free) interactions are important.

Nonanalytic power laws (with rational exponents) for the SK model have been discussed in many different respects, as, for example, for the finite-size cutoff (or finite spin number) dependence [19–21]. One may also mention the exponent of the de Almeida–Thouless line [18]. However, a link to specific critical points has not been made.

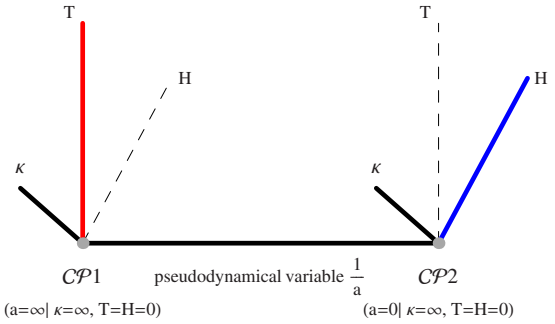

FIG. 1. (Color online) Thermal critical behavior at $\mathcal{CP}1$ versus magnetic-field scaling at $\mathcal{CP}2$: scaling regimes near the two critical points of the SK model at zero temperature, zero field, and infinite replica symmetry breaking. The critical points are separated by the full range of continuously distributed pseudotimes $1/a$. Thick lines indicate the relevant scaling variables.

In the present paper, we report progress in understanding replica symmetry breaking in the Sherrington-Kirkpatrick model [12] as a critical phenomenon; this refers to scaling behavior on one hand and to (numerically determined) fixed-point functions under RSB-order flow $\kappa \to \infty$ on the other. Nonanalytic scaling behavior is described as a function of the inverse RSB order decreasing to zero either together with temperature $T \to 0$, or together with the (homogeneous) external magnetic field. Temperature and field scaling become well separated in the sense that they originate in contributions to the free energy functional $F[q(a)]$ from opposite limits of a pseudodynamic variable $1/a$ (see Ref. [22]), as sketched by Fig. 1 [23].

Critical phenomena are, in general, categorized by universality classes and described by criteria such as global symmetries. Certain details (on shorter range) become irrelevant and suppressed in the regime of divergent correlation lengths. In the early years of the development of phase transition theory and critical phenomena, Kadanoff's pioneering ideas of universality and rescaling, Stanley's scaling theory, and Wilson's renormalization group led to the modern understanding of critical behavior [24]. In recent years the functional renormalization group was advocated to understand better disorder-related criticality [25].

Freezing transitions into spin-glass phases were analyzed in the renormalization framework too, the ordered phase itself remained, however, mysterious, in particular, for the non-mean-field models. In a famous work on scaling in spin glasses, Fisher and Sompolinsky [26] explained the complications of mean-field models (or mean-field regimes of finite-range spin glasses above $d=6$ and $d=8$) and the multiple violations of scaling relations. In particular, they mentioned the violation of temperature-versus magnetic-field scaling within the ordered phase. In a different manner, we encounter this problem and explain a certain decoupling of field from temperature scaling by the presence of two different critical points of RSB in the low-temperature limit.

Crucial questions for a relationship of Parisi's RSB with the Fisher-Huse droplet theory [27] of the ordered phase of real spin glasses (or their reconciliation) stimulated intensive research [28,29]. Since droplet theory is interpreted to govern the ordered phase by a $T=0$ fixed point, it appears desirable to understand RSB as a $T=0$ fixed-point theory too. Attempts have been independently made by several authors and for different physical systems, as the examples of Refs. [22,24,30–32] show.

In previous publications [22,30] we reported the existence of two critical points and of discrete spectra, which survived in the limit of infinite replica symmetry breaking (∞-RSB) for the SK model at $T=0$. This is perhaps surprising, since the ∞-RSB limit is generally known only as the "continuum limit." Indeed, a continuum scaling theory, dealing with the $T \to 0$ limit at $\kappa=\infty$) was published by Pankov [31] recently. Its role and limitation to the temperature-controlled critical point $\mathcal{CP}1$ has been addressed in our previous publication [33] together with a comparison of our work with the much older so-called PaT scaling [34]. In the present paper we do not use Pankov or PaT scaling, but construct a different scaling approach, which includes RSB-order scaling, and is exclusively guided by the theory of critical phenomena. In accordance with previous (naive) functional renormalization-group arguments [30] we analyze the approach to full RSB formation ($\kappa \to \infty$) not only at $T=0$ but also in the (H,T) plane for small values of temperature T and magnetic field H, and as a function of RSB order.

We consider RSB orders, counted by integers $1,2,\ldots,\kappa$, to define equidistant sites, which form a pseudolattice. In analogy with a real-space lattice, which needs to be infinitely large in order to allow for diverging correlation lengths and hence support critical phenomena, the pseudolength cutoff κ must be sent to infinity. The known fact that increasingly higher orders of RSB are needed (for good approximations) as the temperature decreases towards zero implies the role of T as an effective cutoff of nonanalytic behavior in the RSB limit (T playing the role of a symmetry-breaking relevant perturbation in standard critical phenomena). It also suggests the idea of scaling RSB order κ with temperature T. Conversely, a maximum RSB order κ serves as a cutoff of criticality. A speciality of RSB is that it appears in the shape of a pseudodynamical critical phenomenon [22,30], which recalls the celebrated dynamical representation of Sompolinsky [35]. A technically important difference, however, is the absence of a stochastic field. We proposed its use in order to represent couplings to faster degrees of freedom [36].

A scaling theory, near $T=0$ in particular, is important for several different reasons. First, it expresses the numerically determined features of the SK model in a universal form due to scale invariance. This helps to identify model-independent features and places the SK model and its RSB into a wider context. The scaling theory also puts constraints on the shape of an effective field theory. It has the virtue of isolating critical features, which must be represented correctly by an effective theory that simplifies the SK model. The simpler theory should allow one to control generalizations to finite range or other complications, which are far beyond the goal of the present work. Yet, the scaling theory offers a special outlook on a possible scenario of RSB breakdown when the collapse of the spin-glass phase ($T_c \to 0$) eventually combines RSB criticality with the freezing transition.

The paper is organized as follows. Section II describes the basic elements of the present scaling theory. The different sets of scaling variables for both critical points, distinguished

by two opposite pseudodynamical limits, are given. Section III demonstrates how the order parameter function $q(a)$ can be regarded and obtained as a fixed-point function $q^*(a^*)$ under RSB flow $\kappa\to\infty$. Section IV includes and combines finite temperature scaling near critical point $\mathcal{CP}1$ with RSB-order scaling. Scaling functions are obtained, which fit the detailed data of 200 RSB orders, and explain the noncommuting singular limit $\kappa\to\infty$, $T\to 0$. In a similar way, Sec. V includes magnetic-field scaling near $\mathcal{CP}2$. In Sec. VI we present unconventional scaling contributions to the free energy, to the entropy, and internal energy, which are compatible with the numerical self-consistent solutions. In Sec. VII the ground-state energy distribution is given as a function of pseudotime and is also shown as a function of the (normalized) Parisi levels l/κ such that the flow towards an energy-per-level fix-point function results as the RSB order tends to infinity. In Sec. VIII we finally consider pseudodynamic scaling of the order function $q(a)$ in the vicinity of both critical points before concluding with details of $q(a)$ as revealed by its derivatives in Sec. IX.

II. SCALING SCENARIO

We introduce the (RSB-)scaling idea by viewing the formation of full RSB as a critical phenomenon with two critical points in the pseudodynamic limits $a=0$ and $a=\infty$ at $T=0$, $H=0$. We do not *a priori* impose a relationship between the two critical points, but consider the pseudodynamical crossover between them by means of the order function $q(a)$ on $0\leqslant a\leqslant\infty$. Figure 1 illustrates the relative position of the two critical points and the sets of scaling variables near these points.

In particular, one may notice that the dynamical variable $1/a$ and the RSB order κ define a $(1+1)$-dimensional analogy of problems with one time- and one real-space dimension. Since the free energy or internal energy are integrals over all pseudotimes, as, for example, given below in Eqs. (23) and (25), we do not start from a single scaling hypothesis for the free energy F. Instead we construct the scaling hypothesis for each of the two different scaling contributions, originating in these separated critical points. As illustrated by Fig. 1, two different sets of scaling variables should be used in order to match the numerical results.

It is remarkable that temperature- and magnetic-field scaling become decoupled, because they belong to different scaling regimes. Scaling with the respect to the order κ of RSB measures the approach of the equilibrium solution at $\kappa=\infty$ (full RSB) and therefore can be viewed as a kind of nonequilibrium dynamics (in the sense that each finite order is unstable towards higher RSB orders). Thus an element of dynamic scaling is contained. Using the pseudotime $1/a$ as an additional scaling variable, we analyze the order function $q(a;T,H)$ and its pseudodynamic scaling behavior. A dynamic crossover between the two critical points $\mathcal{CP}1$ and $\mathcal{CP}2$ is then described by means of $q(a)$. Moreover, the order function is evaluated as a fixed-point function of the RSB flow letting $\kappa\to\infty$.

The present scaling theory is then fitted to high precision numerical data, which were obtained recently for the

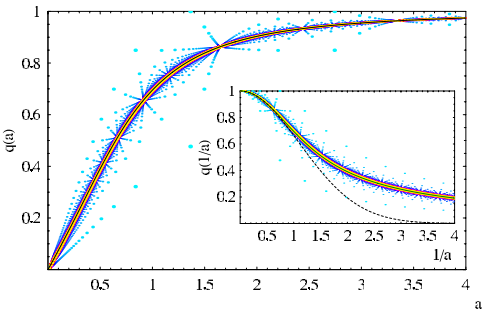

FIG. 2. (Color online) The main figure and inset present a wide-scale overview of all $(T=0,\ H=0)$ self-consistent solutions $\{a_l^{(\kappa)},q_{l+1}^{(\kappa)}\}$ and $\{a_l^{(\kappa)},q_l^{(\kappa)}\}$, where $l=1,\ldots,\kappa$ for each RSB order $\kappa=1,2,\ldots,200$. The RSB flow from small orders κ (the dot size decreases with RSB order κ) to the highly dense regime $\kappa=200$ demonstrates how the true order function $q(a)$ (black curve) is approached by the densely spaced $q_{l+1}(a_l)$ from below and by $q_l(a_l)$ from above. The inset shows the corresponding $\{1/a,q\}$ data and the function $q(1/a)$ they converge to. The shape near $\tau\equiv\frac{1}{a}=0$, $(\mathcal{CP}1)$ is almost Gaussian [dashed black curve: $\exp(-0.41/a^2)$] but crosses over for moderate and small $1/a$ to strongly non-Gaussian and a tail behavior $q(\tau)\sim 1/\tau$.

Sherrington-Kirkpatrick model given by the Hamiltonian

$$\mathcal{H}=\sum_{i<j}J_{ij}s_is_j-H\sum_i s_i,$$

with quenched, infinite-ranged, and Gaussian-distributed random couplings J_{ij} (with variance J^2/N) between classical spins $s_i=\pm 1$. The method was described in Ref. [33] and will not be described again in this paper. It allowed one not only to go beyond earlier high-order studies [22], but also contained new analytical elements. As a consequence we are able to predict the values of critical exponents, evaluate amplitudes, and calculate analytical models of various scaling functions including cases with very singular crossover.

The numerical material includes the self-consistent solutions in all orders of RSB up to (i) the current maximum of $\kappa=200$ RSB at $T=0$ and $H=0$, (ii) 50 orders for a dense grid of finite temperatures in the range $0\leqslant T\leqslant 0.3$ for $H=0$, and (iii) 20 orders of RSB for a dense grid of finite magnetic fields $0\leqslant H\leqslant 0.5$ at zero temperature.

We note that all energies are given in units of J.

III. $T=0$-ORDER FUNCTION AS A FIXED-POINT FUNCTION $q^*(a^*)$ IN THE RSB LIMIT $(\kappa=\infty)$

The idea of finding the $T=0$-order function as a fixed-point function in the RSB limit arose from renormalization-group arguments as designed in Ref. [30]. It reemerges now in a literally obvious way when we plot in Fig. 2 the whole set of numerical self-consistent solutions $\{a_l^{(\kappa)},q_{l+1}^{(\kappa)}\}$ (and $\{a_l^{(\kappa)},q_l^{(\kappa)}\}$) for $l=1,\ldots,\kappa$ of all evaluated RSB orders $\kappa=1,2,\ldots,200$. These data become dense for large κ and approach the desired order function $q(a)$ in the limit $\kappa\to\infty$, which can be viewed as a fixed-point function $q^*(a^*)$.

The unusual form $q^*(a^*)$ can be justified as follows: the parameters $a_l^{(\kappa)}$ and $q_l^{(\kappa)}$ can be viewed as functions of the

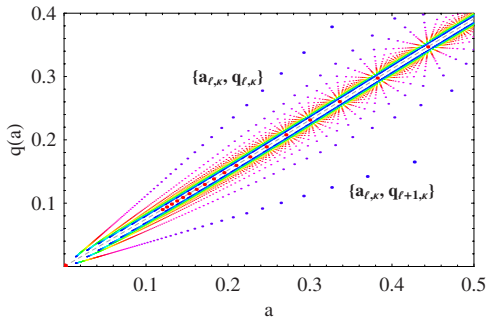

FIG. 3. (Color online) Self-consistent $\{a,q\}$ data in the small-a regime are shown for all $\kappa=1,2,\ldots,200$ RSB orders, together with an analytical model function $q(a)$ (dashed gray line). Solutions $\{a_{l,\kappa},q_{l+1,\kappa}\}$ (above the line) and $\{a_{l,\kappa},q_{l,\kappa}\}$ (below) approach fixed points under RSB flow obeying the constraint $\kappa=\kappa(l)$, l level number. Fixed-point examples for $\kappa=l(m+1)/m-k/m-1$, $23\geqslant m\geqslant 6$ and k integer are shown (big red dots along the dashed line) including the fixed point (0,0) (RSB flow along $\kappa=l+k$). The analytical model function for $q(a)$ matches well all fixed points.

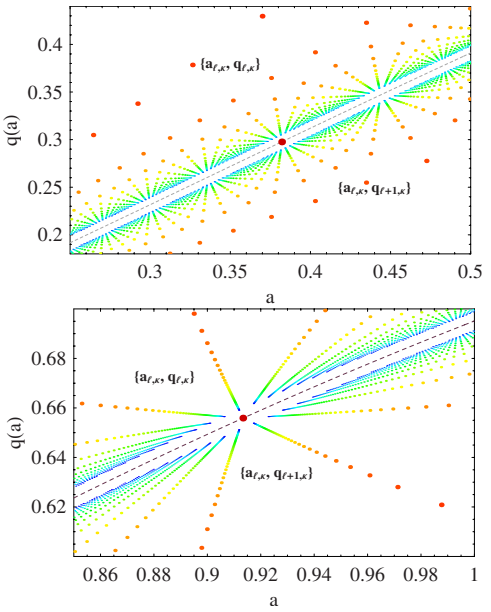

FIG. 4. (Color online) Two examples of alignment of solutions $\{a,q\}$ under constrained RSB flow with $\kappa(l)$ towards two fixed points (big dark-red dots): (upper figure) $p^*_{m=7,n=6}\equiv(a^*,q^*)_{m=7,n=6}=(0.3820,0.2976)$ and (lower figure) $p^*_{m=3,n=2}\equiv(a^*,q^*)_{3,2}=(0.9133,0.6559)$. Padé-line intersections, shown for $p^*_{7,6}$ in Fig. 5 and for a large-a fixed point in Fig. 6, determine the fixed points. A closer look shows that RSB fix points lie dense and yield a fixed-point function, well approximated by the model function $q(a)$ (dashed gray).

continuous variable $l/\kappa\to\zeta$ in the $\kappa\to\infty$ limit. The fixed-point solutions $a^*(\zeta)$ and $q^*(\zeta)$ can be combined by eliminating the variable ζ, which results in the special form $q^*(a^*)$, where the variable itself is made up from continuously distributed fixed points. In the following we use $q(a)$ and $q^*(a^*)$ synonymously and distinguish them only if necessary.

At finite large orders one may define interpolating functions $q_{l+1}(a_l)\to q_<(a)$ and $q_l(a_l)\to q_>(a)$, which yield lower and upper bounds for the exact solution $q(a)\equiv q^*(a^*)$ at each value of a. Figure 2 illustrates that this channel between lower and upper bound becomes extremely small for high orders $\kappa=O(10^2)$. An illustration of the exact $q(a)$ being confined within such a channel as the RSB order κ increases towards infinity, is provided in a more detailed way by zooming different regions of crossover between $\mathcal{CP}1$ and $\mathcal{CP}2$ in Figs. 3 and 4.

Figure 2 moreover shows deviations of $q(1/a)$ from Gaussian behavior, which is a good approximation for small $1/a$. In both representations $q(a)$ and $q(1/a)$ it illustrates the existence of special lines, which terminate obviously in fixed points—in fact there is a hierarchy of fixed points lying dense on the interval $0\leqslant a\leqslant\infty$. We shall make explicit use of these fixed points below.

Indeed, 200 calculated orders of RSB for $T=0$ already yield an almost continuous function $q_l\left(\frac{a_l+a_{l+1}}{2}\right)$, which finally turns into $q(a)$ in the RSB limit. Our previously published analytical model function [22] satisfies almost perfectly this constraint. Its form

$$q_{model}(a)=\frac{a}{\sqrt{a^2+w(a)}}{}_1F_1\left(\alpha,\gamma,-\frac{\xi^2}{a^2+w(a)}\right) \qquad (1)$$

models even the full crossover regime. The monotonically decreasing "mass" function $w(a)$ assumes a small constant $w(0)\approx 0.067$, which prevents potentially nonanalytic small-a behavior for arbitrary parameters α,γ, and guarantees a strictly linear $q(a)$ behavior in accordance with our high-order data. In the crossover regime between these two dynamic critical points, $w(a)$ can be modeled (using three parameters) to depress the maximum error of $q(a)$ below $O(10^{-4})$ at each pseudotime. A unique choice of $w(a)$ is not yet found, but excellent fits are obtained with $w(a)$ monotonically decreasing from $w(0)\approx 0.067$ to $w(\infty)=0$ together with the parameters $\alpha\approx 0.558$, $\gamma\approx 1.87$, $\xi^2\approx 1.41$. Using the high-order data we have thus been able to improve the analytic approximation of the $T=0$ order function $q(a)$.

A. Fixed points calculated from the RSB flow towards $\kappa=\infty$

The full set of self-consistent solutions for order parameters q_l and (T-normalized) Parisi box sizes $a_l\equiv m_l(T)/T|_{T=0}$ can be described by matrix elements $p_{l,\kappa}\equiv\{a_{l,\kappa}\equiv a_l^{(\kappa)},q_{l,\kappa}\equiv q_l^{(\kappa)}\}$ labeled by RSB order κ and level number l. Since the number of q_l parameters exceeds by one the number of a_l parameters (in each order of RSB), a second complementary set of matrix elements $\tilde{p}_{l,\kappa}\equiv\{a_{l,\kappa},q_{l+1,\kappa}\}$ should also be taken into account. These points $p_{l,\kappa}$ and $\tilde{p}_{l,\kappa}$ are displayed in the Figs. 2–6 and observed to approach the exact $q(a)\equiv q^*(a^*)$ along characteristic lines given below by Eq. (2) as $\kappa\to\infty$ (p from above and $\tilde{p}$ from below $q(a)$, since $q_{l+1,\kappa}<q_{l,\kappa}$).

The set of all RSB solutions up to a maximum order κ, as plotted in Fig. 2 with a cutoff at $\kappa=200$, is then described by two triangular matrices with entries $\{a_{l,\kappa},q_{l,\kappa}\}$ (or with $\{a_{l,\kappa},q_{l+1,\kappa}\}$); the level numbers l run from 1 to κ for each RSB order κ.

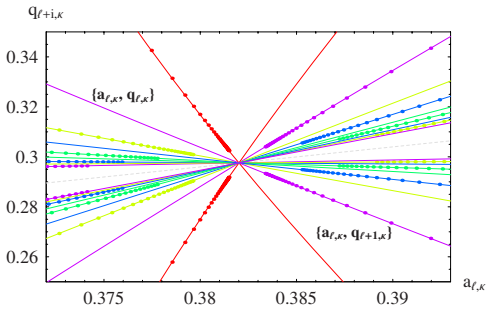

FIG. 5. (Color online) Padé approximants matching the RSB flow of discrete solutions (dots) $q_{l+i,\kappa}$ at $a_{l,\kappa}$ (for $1 \leqslant \kappa \leqslant 200$ and $i=0,1$) along $\kappa=\frac{7}{6}l-k/6-1$ for integers $k=-4,-3,\ldots,4$, with initial values $l_0=6+k$, $\kappa_0=6+k$, and $\Delta l=6$. All lines join in the RSB fixed point $p^*_{7,6}=(0.3820,0.2976)$ as $\kappa\to\infty$. (Padé curves are displayed here without termination at the fix point.)

Along infinitely many lines in (l,κ) space—the leading ones are very clearly visible in Figs. 3 and 4 (and shown as calculated in Figs. 5 and 6)—we observe very smooth behavior of slowly changing parameters $(a_{l,\kappa},q_{l,\kappa})$, which allow low-order Padé approximants to match these data and to join in fixed points p^* of the order function curve for $\kappa=\infty$. A special case is the origin where the best Padé approximations (for example, obtained for $l=\kappa$ in Fig. 2) deviate only by $O(10^{-13})$ from the exact value (0,0) in the RSB limit.

Typical examples of such characteristic lines in (l,κ) space can be given by the linear relation among the labels

$$\left\{ l+k, \kappa = \frac{m}{n} l + k - 1 \right\} \tag{2}$$

(viewing $l \geqslant l_{min} \equiv l_0 = n$ as the running index) with steps of $\Delta l=n$ and m,n,k integer valued. The choice of m/n selects one fixed point of the RSB flow as $\kappa\to\infty$ with $l\to\infty$. Steps of $\Delta l=n$ are required to generate integer values for κ (otherwise we would not have numerical data). The integer k distinguishes different lines, which all meet in the same fixed point. Thus the fixed point (a^*,q^*) is labeled by m and n or just by the rational number m/n. We have evaluated more

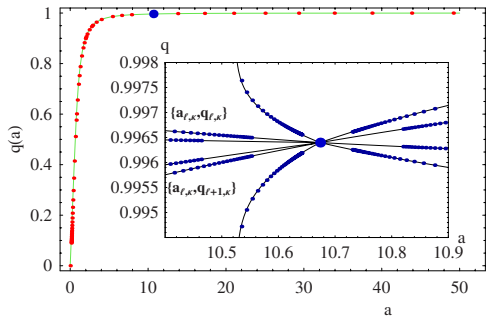

FIG. 6. (Color online) The inset displays a fixed-point example in the $a \gg 1$ regime with nonlinear RSB flow along $\kappa=6l+k$, $k=-2,-1,\ldots,2$, modeled by Padé curves ending in a large-a fixed point. Its position (big dot) at {10.6736,0.9964} is also shown in the main figure with respect to a set of 50 other fixed points (small dots), which agree well with the model function $q(a)$ as shown in the main figure.

than 50 fixed points belonging to the exact order function $q(a)$. The higher n the larger must be the steps Δl, hence one needs higher orders of RSB to find enough data points for reasonable curve fitting through these points. This is one limitation of the method, but the almost linear character of a large number of these lines allows one to calculate, in principle, a number of fixed points much larger than the order of RSB.

B. Discrete spectra in the $\kappa=\infty$ RSB limit at zero temperature

While the fixed-point functions can be derived for all pseudotime values $1/a$, the points $a=0$ and $a=\infty$ remain special limits. In a recent paper [22] we have shown that infinitely large subclasses of certain self-consistent parameter ratios remain discrete at $T=0$ or $H=0$ even in the continuum limit. These discrete levels reside in the limits $a=0$ and $a=\infty$ when $\kappa=\infty$. Finite temperatures lift the discrete spectrum at $a=\infty$ into the continuum, while a magnetic field has a similar effect on the discrete levels at $a=0$. The ratios assume the value 1 then. The discrete spectra therefore emphasize the critical nature of the points $a=0$ and $a=\infty$. We present in the following subsections new results for these $T=0$ levels of parameter ratios and, in Sec. IV, describe their singular finite T crossover.

1. Level distribution at $\mathcal{CP}2$

At the critical point $\mathcal{CP}2$ the subclass of small self-consistent parameters q_i and a_i, which vanish in the ∞-RSB limit (and condense into $\mathcal{CP}2$), obey

$$\frac{q_{\bar{l}+2}}{q_{\bar{l}+1}} = \frac{2l-1}{2l+1} \quad \text{and} \quad \frac{a_{\bar{l}+2}}{a_{\bar{l}}} = \frac{l}{l+1}, \tag{3}$$

with $\bar{l} \equiv \kappa - l$ and $l=1,2,\ldots,l_{max} \ll \kappa$; thus the ratios of these parameters are discrete and almost equidistant [22]. Recurring these relations to the smallest parameters of each RSB order κ, hence to $q_{\kappa+1}$ and a_κ, respectively, we obtain

$$q_{\kappa+1-l} = (2l+1) q_{\kappa+1}, \quad a_{\kappa-l} = (l+1) a_\kappa. \tag{4}$$

The RSB flow of numerical data up to 200 RSB allow one to conclude that these minimal parameters vanish like

$$q_{min} \equiv q_{\kappa+1} = \frac{1.03059}{\kappa} + \frac{1.31705}{\kappa^2} + O(1/\kappa^3), \tag{5}$$

$$a_{min} \equiv a_\kappa = \frac{2.77275}{\kappa} + \frac{3.54347}{\kappa^2} + O(1/\kappa^3). \tag{6}$$

The discretized slope of the order function in the point $a=0$, assumes the 200 RSB value

$$\frac{q_{\bar{l}} - q_{\bar{l}-1}}{a_{\bar{l}} - a_{\bar{l}-1}} = \frac{2q_{\kappa+1}}{a_\kappa} \simeq 0.74345, \tag{7}$$

or, by Padé approximation of the RSB flow and extrapolation to ∞-RSB, one obtains

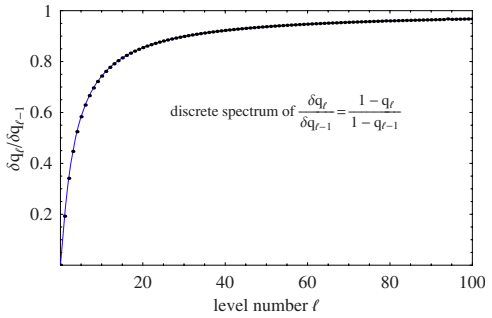

FIG. 7. (Color online) The discrete ratios $\delta q_l/\delta q_{l-1}$ of $\delta q_l \equiv 1-q_l$, which vanish for $\kappa \to \infty$ at $T=0$, as obtained by Padé extrapolation to the RSB limit, plotted versus the level number l.

$$q'(0) = 2 \lim_{\kappa\to\infty} \frac{q_{\kappa+1}}{a_\kappa} \simeq 0.743\,368. \tag{8}$$

As the calculation of fixed points of $q(a)$ in the linear small-a regime shows, this agrees with the slope of the continuous $q(a)$ for $a \to 0$. The slope of the order function in $\mathcal{CP}_2$ provides a quite accurate constraint for the order function

$$q'_{model}(a=0) = \frac{1}{\sqrt{w(0)}} {}_1F_1\left(\alpha, \gamma, -\frac{\xi^2}{w(0)}\right) \simeq 0.743\,368. \tag{9}$$

2. Level distribution at $\mathcal{CP}1$

In the large-a limit the characteristic features are discrete spectra of $1-q_l$ ratios, which are shown in Fig. 7. In addition, Fig. 8 shows that the $\frac{1}{a^2}$ coefficient of the almost continuous order function converges towards 0.41 except for the largest a levels. At zero temperature the order function differs from 1 by $0.41/a^2$. Thus, according to the large-a expansion of our analytical model, the expansion coefficient is constrained to satisfy

$$q(a) = 1 - \frac{\alpha\xi^2}{\gamma}\frac{1}{a^2} + O(1/a^4) = 1 - 0.41\frac{1}{a^2} + O(1/a^4), \tag{10}$$

putting a constraint on $\alpha\xi^2\gamma$. Further constraints can be found from very precise numerical characteristics; it is planned to use this analysis to narrow down the choice of an analytical order function model.

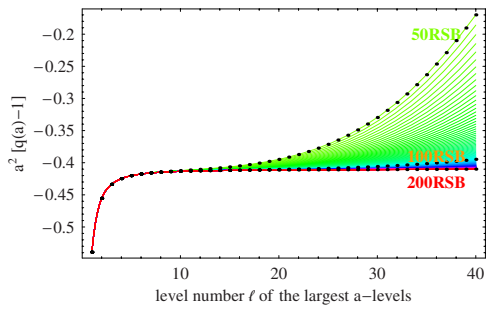

FIG. 8. (Color online) The figure shows convergence of the large-a behavior of $a^2[q(a)-1]$ towards ≈ -0.41. Levels belonging to the discrete spectrum at $a=\infty$ show a deviation.

The discrete spectrum yields a coefficient, which differs notably from this value, as one can see from Fig. 7 (right) for the leading divergent a_l parameters.

C. Approach of equilibrium at $T=0$: Leading and subleading scaling contributions

The nonequilibrium susceptibility χ_1 is a characteristic quantity measuring the distance from the equilibrium solution at $\kappa=\infty$. The entropy had been seen [33] to vanish like the square of χ_1. The numerical solutions [33] for χ_1, evaluated for all 200 leading RSB orders, are well fitted by the $T=0$ form

$$\begin{aligned}\chi_1(\kappa, T=0) &\cong \frac{0.86}{(\kappa_0+\kappa)^{5/3}} + \frac{1.85}{(\kappa_0+\kappa)^4} + \cdots \\ &= 0.86\kappa^{-5/3} - 1.83\kappa^{-8/3} + 3.12\kappa^{-11/3} \\ &\quad + 1.85\kappa^{-4} + \cdots,\end{aligned} \tag{11}$$

with $\kappa_0 \cong 1.278$. As discussed in Ref. [33] the numerical uncertainty of $O(10^{-6})$ in the exponent is so small that the expectation of a rational-valued exponent due to one dimensionality leads to the firm prediction of $\chi_1 \sim \kappa^{-5/3}$. The quality and density of the numerical results is even high enough to predict the subleading correction and the amplitudes as well.

IV. FINITE TEMPERATURE SCALING NEAR THE CRITICAL POINT $\mathcal{CP}1$ ($a=\infty$, $T=0$, $H=0$)

Naturally one would like to start with a scaling hypothesis for the free energy F. However, the SK model has two critical points at $T=0$ and the free energy picks up contributions from both; in the RSB limit, it can be expressed by integrals over an entire crossover range from $a=0$ ($\mathcal{CP}_2$) to $a=\infty$ ($\mathcal{CP}_1$) involving the order function $q(a)$.

Thus it turns out useful to start with the scaling behavior of the self-consistent parameters a_l and q_l, which teaches us how to embed scaling into the order function $q(a,T)$ mediating the crossover between the two critical regimes. Finally, by expressing free energy and internal energy in terms of the order function, and by linking the entropy with the nonequilibrium susceptibility, we shall arrive at consistent scaling predictions for F, U, and S below.

Let us begin with temperature-normalized block size parameters

$$a_l(\kappa, T) \equiv \frac{m_l(\kappa, T)}{T}, \tag{12}$$

where we consider first scaling in the (κ, T) plane for fixed label l. We must analyze the singular behavior near the critical point $\mathcal{CP}_1$, where diverging $a_l(\kappa, T=0) \to \infty$ for $\kappa \to \infty$ lead to discretely spaced ratios $a_l(\infty,0)/a_{l-1}(\infty,0)$ in the ∞-RSB limit. We identified the large-order power-law divergence

$$a_l(\kappa, T=0) \sim \kappa^{5/3}, \quad \kappa \to \infty \tag{13}$$

for the subclass of large parameters a_l (their number also grows to infinity as $\kappa \to \infty$).

The linear temperature decay of all Parisi box sizes $m_l(\kappa, T) \sim T$ holds for all *finite* RSB orders, but not all m's should vanish in the RSB limit at zero temperature, since the break point is not expected to be at $m_1=0$ (even in the $T \to 0$ limit [37,38]). Thus, one should describe noncommuting limits $T \to 0$ and $\kappa \to \infty$ properly.

The Taylor series, valid as a low-temperature expansion for any fixed finite RSB order,

$$m_l(\kappa, T) \equiv a_l(\kappa, T)T = a_l(\kappa, 0)T + a_l'(\kappa, 0)T^2 + O(T^3), \tag{14}$$

will anyway break down for those levels l for which the expansion coefficients diverge as $\kappa \to \infty$. In accordance with the anomalous power law (13) it will be shown below by means of the fixed-point order function that the correct scaling form for this $\mathcal{CP}_1$-divergent parameter subclass reads

$$a_l(\kappa, T) = \kappa^{5/3} f_{a_l}(T/\kappa^{-5/3}), \tag{15}$$

where the scaling function is well approximated by a low-order (2, 3) Padé series [one may also use a (1, 2) or (3, 4) series]

$$f_{a_l}(x) = \frac{c_{0,l} + c_{1,l}x}{1 + d_{1,l}x + d_{2,l}x^2}. \tag{16}$$

This form fits well the available finite T data up to 50 RSB and satisfies

$$f_{a_l}(0) = c_{0,l} \text{ finite} \quad \text{and} \quad f_{a_l}(x) \sim \frac{1}{x} \quad \text{for } x \to \infty. \tag{17}$$

The crossover line can be described by the characteristic (crossover) temperature

$$T_1(\kappa) \sim \kappa^{-5/3}. \tag{18}$$

Beyond the crossover line, for temperatures $T \gg T_1(\kappa)$, the box sizes $m_l(x) = x\, f_{a_l}(x)$, which belong to the $\mathcal{CP}1$-divergent subclass of a_l's, approach finite temperature-independent values. One obtains

$$\lim_{x \to \infty} m_l(x) = c_{1,l}/d_{2,l}. \tag{19}$$

While direct fits of our numerical data yield already a crude estimation of $m_1(\infty)$ for the break point, it was mentioned in Ref. [33] that 50 RSB is not sufficient to determine the break point for arbitrary low temperatures. Yet, for $T=0.015$ a reliable break point value was determined by another procedure.

Here we are interested to obtain a good estimation of the break point in close connection with the scaling picture. Therefore we employ the fixed-point method and indeed succeed in finding a good approximation down to even lower temperatures and also answer the question whether the limit $m_l(\infty)$ in Eq. (19) shows a level index dependence or not. For finite m_l an l dependence would have implied a discrete distribution. We shall find in Sec. IV A that all ratios become level independent in the large x limit

$$\frac{m_l(x)}{m_{l-1}(x)} = \frac{a_l(x)}{a_{l-1}(x)} = \frac{f_{a_l}(x)}{f_{a_{l-1}}(x)} \to 1 \quad \text{for } x \to \infty. \tag{20}$$

The crossover from discrete parameter spectra for $T \ll T_1(\kappa)$ to the continuum on the other side of the crossover line, for $T \gg T_1(\kappa)$, is a rather singular effect mediated by the scaling function. We introduced above a scaling function, which allows one to suppress the discrete spacing between q and a parameters as one moves through the crossover line $T_1(\kappa) \sim \kappa^{-5/3}$.

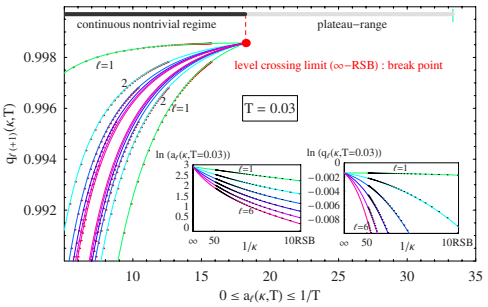

FIG. 9. (Color online) The main figure shows the RSB flow of $\{a_l(\kappa), q_l(\kappa)\}$ (above) and of $\{a_l(\kappa), q_{l+1}(\kappa)\}$ (below), for each of the six highest parameter levels ($l=1, \ldots, 6$) at fixed temperature $T=0.03$. Padé approximations model the flow $\kappa \to \infty$ by extrapolation. $\kappa=\infty$ is reached in the level crossing point $\mathcal{LCP} = \{a_k(\kappa) \cong 18.226, q_k(\kappa) \cong 0.9986\}$, which separates plateau regime $\mathcal{LCP} \leqslant a \leqslant 1/T$ from the ∞-RSB continuum $0 \leqslant a \leqslant \mathcal{LCP}$. The Parisi box size $m(T=0.03)=0.5467$ is the break point value. The inserts illustrate that q_l and a_l levels meet in the $\mathcal{LCP}$ for $\kappa=\infty$.

A. Forbidden level crossing at finite temperatures determines the break point

We employ now the RSB fixed-point technique to extract approximate values for the break point for rather low temperatures.

For this purpose, we consider fixed finite temperatures T and fixed level numbers l (down to lowest T and l small to catch the diverging-a subclass near $\mathcal{CP}1$) and study the RSB flow of the solutions $\{a_l(\kappa), q_l(\kappa)\}$, and also those of the complementary type $\{a_l(\kappa), q_{l+1}(\kappa)\}$, from low orders up to $\kappa=50$ as illustrated by Fig. 9 for an arbitrarily picked temperature $T=0.03$. Padé approximants fit the RSB flow well and these extrapolated curves meet precisely in the same point. These curves would cross each other, but then violate the reality condition of the self-consistent method beyond the level crossing point. We consider the level crossing point therefore as the limit of the nontrivial part of the order function, hence as the break point.

The scenario remains the same for arbitrary fixed temperatures; only the extrapolation range increases with the level number and therefore becomes less accurate for smaller temperatures. Yet reliable solutions were obtained down to temperatures $T \approx 0.005$. The figure inset emphasizes the fact

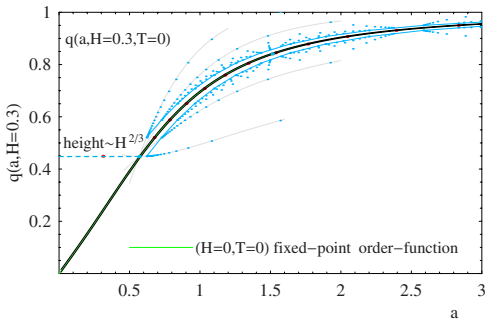

FIG. 10. (Color online) Upper and lower bounds of the order functions are shown for {20 RSB, $H=0.3$} and in 200 RSB for zero field. For comparison the $H=0$ fixed-point order function (green) is included. The interpolated order function and two fixed points for finite field $H=0.3$, as obtained from the 1–20 RSB flow extrapolated to $\kappa=\infty$ (light-gray lines), almost coincide with the $H=0$ result above the plateau value. The fixed point at $a^*_{pl}=0.568$, $q^*_{pl}=0.448$ defines the plateau cutoff of $q(a)$ in the finite field $H=0.3$.

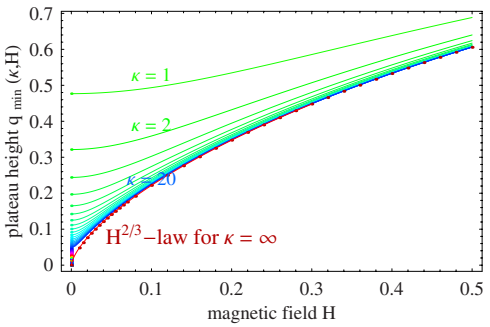

FIG. 11. (Color online) Numerical data for the magnetic-field range $0<H\leqslant 0.5$ are shown from first to 20th order of RSB (green). Dots (dark red) show the plateau-height small-q cutoff obtained from the fixed-point order function. At $H=0$ dots show the calculated orders up to 200 RSB for comparison. The RSB flow for $q_{min}(\kappa,H=0)$ is given by a $1/\kappa$ law, while $q_{min}(\kappa=\infty,H)$ obeys an $H^{2/3}$ law.

that the solutions indeed reach the level crossing point as $\kappa\to\infty$.

Approaching zero temperature and the RSB limit along the crossover line, x fixed, with $T_1(\kappa)\sim\kappa^{-5/3}$, leads to a discrete set of different Parisi box sizes $m_l(\kappa=\infty,T=0)$.

B. Nonequilibrium susceptibility χ_1

The scaling form of the nonequilibrium susceptibility $\chi_1(\kappa,T)$ can be given in terms of a scaling function f_1 by

$$\chi_1(\kappa,T)=\kappa^{-5/3}f_1(T/\kappa^{-5/3}), \tag{21}$$

where $f_1(x)\sim x$, $x\to\infty$, and $f_1(0)\cong 0.86$, reproduces the data and the leading κ decay at $T=0$, as in Eq. (11).

V. MAGNETIC-FIELD SCALING AT CRITICAL POINT $\mathcal{CP}2$ (DIVERGING PSEUDOTIMES $1/a\to\infty$)

The magnetic-field dependence at $T=0$ is expected to yield a plateaulike cutoff of the order function of similar shape as described in the Parisi form $q(x)$. We study now the field dependence of the smallest-order parameter $q_{\kappa+1}(H,T=0)$ in κth order of RSB. Twenty orders of RSB turn out to be enough to extract the exponent describing the decay of $q_{\kappa+1}$ as the order of RSB tends to infinity. Guided by the results for finite temperature, where one single nontrivial rational exponent appeared, we observe an exponent $2/3$ to provide a reasonable picture for extrapolation towards ∞-RSB (Fig. 10).

We first identify the $q_i\sim\kappa^{-1}$ law for (infinitely many) order parameters, which vanish as $\kappa\to\infty$. The scaling hypothesis for (κ,H) scaling [39], valid for the vanishing-order parameters $q_i(\kappa,H)$, can be formulated as

$$q_i(\kappa,H,T=0)=\frac{1}{\kappa}f_i\left(\frac{H^{2/3}}{1/\kappa}\right), \tag{22}$$

with $f_i(0)\neq 0$ and $f_i(x\to\infty)\sim x$.

The numerical procedure chosen in order to arrive at this proposal has been to extrapolate to ∞-RSB the smallest q_i values at fixed nonvanishing small magnetic fields. The higher the field the less orders of RSB are needed (similar as in the case of finite temperatures). Twenty steps of RSB generate almost exact results down to $H\approx 0.15$. Extrapolation of the RSB flow is hence reliable down to much smaller field values, where one has already entered the critical regime. Thus many RSB fixed-point values (at $\kappa=\infty$) are well approximated and can be used to match a power-law with respect to the magnetic field. In this way the magnetic-field exponent of Eq. (22) is found to differ only by 0.003 from the value $2/3$, which led to the assumption that this rational number is exact (Fig. 11) .

VI. SCALING BEHAVIOR OF THE FREE ENERGY F, INTERNAL ENERGY U, AND ENTROPY S

Low-temperature expansions of internal energy U, entropy S, and the free energy $F=U+TS$ were reported in the framework of our high-order RSB analysis, and found in agreement with already known results. In the present context of scaling theory, we also look for scaling of RSB parameters together with temperature and also small field variation. A useful way to study the RSB flow in terms of κ scaling is by invoking the internal energy formula at $T=0$ and $H=0$,

$$U(\kappa,T=H=0)=-\chi_1-\frac{1}{2}\sum_{l=1}^{\kappa}a_l(q_l^2-q_{l+1}^2) \tag{23}$$

$$\Rightarrow\lim_{\kappa\to\infty}U(\kappa,0)=-\frac{1}{2}\int_0^\infty da[1-q(a)^2]. \tag{24}$$

The summation includes contributions from both critical points and from the crossover regime in between. Consequently, one cannot expect to obtain scaling laws from a single hypothesis imposed on the total free energy. The problem has more in common with critical dynamics, however, with two critical points in the long pseudotime limit $(1/a\to\infty)$ and in the short pseudotime limit $(1/a\to 0)$.

As reported in Ref. [33] the free energy has a low T expansion in the RSB limit given by $F=F(T=0)-S(T=0)T$

$+\Sigma_{k=2} f_k T^k$, where the leading temperature behavior is $F(\kappa=\infty,T)-F(\infty,0)\sim T^3$. The leading large-$\kappa$ correction of the $T=0$ free energy has also been reported to decay like κ^{-4}.

In the large-a regime, temperatures scale like $\kappa^{-5/3}$ and hence the large-a scaling contribution is $\delta F\sim\kappa^{-5}$. Thus the leading temperature dependence belongs to a subleading $\delta F\sim\kappa^{-5}$ correction.

We attempt to distinguish singular scaling contributions from both critical points from the nonsingular contributions to the free energy. The small-a-regime contribution can be estimated from

$$F(\kappa=\infty,T=0)=U(\kappa=\infty,T=0)$$
$$=E_0(H)=-\frac{1}{2}\int_0^\infty da[1-q^2(a)]-M(H)H, \tag{25}$$

where $M(H)$ denotes the field-generated magnetization. Recalling the small-a expansion of the order function, $q(a)\sim a-\text{const}\,a^3+O(a^5)$, one must expect an $H^{10/3}$ contribution from the plateau regime, which implies also an $O(\kappa^{-5})$ contribution. The free energy data are compatible with an $H^{10/3}$ small field scaling part.

It must be concluded that the leading correction κ^{-4} must originate in the intermediate a regime (not yet identified in detail). It can, after all that was said before, not be assumed to be a scaling contribution. We should therefore attribute it to the regular free energy part.

The entropy was found to obey [33]

$$S(\kappa,T=H=0)=-\frac{1}{4}\chi_1(\kappa,T=H=0)^2.$$

It is known that only the large-a regime near $\mathcal{CP}1$ is responsible for the leading κ behavior of χ_1 at zero temperature, hence this holds also for the entropy $S(T=0)$. Since thermal behavior is also caused by the $\mathcal{CP}1$ contributions, we can therefore claim that the scaling contribution to the entropy obeys

$$S_s(\kappa,T)=\kappa^{-10/3}f_S(T^2/\kappa^{-10/3}), \tag{26}$$

with $f_S(x)=-0.72x$ (see Ref. [33]) for $x\to\infty$ and $f_S(x)\cong-0.185$ for $x\to 0$. Thus the entropy contributes to the leading $O(T^3)$ low-temperature correction of the free energy. This TS term contributes again only a subleading correction $\delta F\sim\kappa^{-5}$ from the large κ-scaling regime.

Let us recall the large-κ dependence of the free energy at zero temperature, well described by the optimal fitting form

$$F(\kappa,T=0)=F(\infty,0)+\frac{c_4}{(\kappa+\kappa_0)^4}+\frac{c_5}{(\kappa+\kappa_0)^5}+\cdots,$$

where excellent Padé fits yield the constant $\kappa_0=1.28$. The leading correction κ^{-4} does neither originate from the scaling regime near $\mathcal{CP}1$ nor from that near $\mathcal{CP}2$, and hence must be expected not to scale. We therefore consider it as part of a regular F contribution $F_{reg}(\kappa,T,H)$.

Thus we propose that the free energy consists of a sum of a regular and of two singular parts, where the latter ones scale according to whether they are $\mathcal{CP}1$ or $\mathcal{CP}2$ critical.

As a consequence of this two-critical-point picture and in agreement with the numerical data, we separate two singular contributions, which offer different scaling behavior, from a regular part F_{reg} by

$$F(\kappa,T,H)=F_{reg}(\kappa,H,T)+F_s^{(\mathcal{CP}1)}(\kappa,T)+F_s^{(\mathcal{CP}2)}(\kappa,H), \tag{27}$$

where the magnetic-field controlled critical point $\mathcal{CP}2$ and the temperature-controlled critical point $\mathcal{CP}1$ contribute, respectively,

$$F_s^{(\mathcal{CP}1)}(\kappa,T)=\kappa^{-5}f_{cp1}(T/\kappa^{-5/3}), \tag{28}$$

and

$$F_s^{(\mathcal{CP}2)}(\kappa,H)=\kappa^{-5}f_{cp2}(H^{2/3}/\kappa^{-1}), \tag{29}$$

with $f_{cp1}(x)\sim x^3$, $f_{cp2}\sim x^5$ for $x\to\infty$ and both finite for $x\to 0$. This claim refers to the leading scaling behavior at $\mathcal{CP}1$ and $\mathcal{CP}2$; corrections with analytic T dependence near $\mathcal{CP}2$ and analytic field-dependent corrections near $\mathcal{CP}1$ may occur.

A contribution $-\frac{1}{2}\chi(\kappa)H^2$ term, which yields the linear equilibrium susceptibility from $-\partial_H^2 F$, belongs to the regular part F_{reg} with $\chi(\kappa\to\infty,T<T_c)=1$.

It is interesting trying to translate the given power laws into scaling with the number N of spins for the finite N SK models [40], which corresponds to a finite-size system with $N=L^d$, d denoting the real-space dimension. Scaling with L or N delivered a leading correction $\sim N^{-2/3}$ for the finite SK model [19,20]. If we would assume scaling of the leading correction κ^{-4} with N, a scaling function depending on $N^{-1/6}/\kappa^{-1}$ would result [41,42]. However, this rests on the assumption that the leading $N^{-2/3}$ energy correction arises from the entire a regime. Many open questions seem to show up here.

VII. FIXED-POINT DISTRIBUTIONS

A. Ground-state energy E_0

We can extract more detailed information from our numerical analysis of RSB in the SK model [22,33] beyond the calculation of the global ground-state energy. The RSB flow of the energy-level distribution and naturally the energy density $\epsilon_0(a)$ as a function of pseudotimes can be given. In the latter case, a test of our analytic order function model against the numerical results [33] is provided by the use of $q(a)$ and of $q'(a)$. Both are required in the ground-state energy formula in Eq. (25) according to

$$E_0=\int_0^\infty da\,\epsilon_0(a)=-\int_0^\infty daaq'(a)q(a). \tag{30}$$

Using the analytic form (3) and high RSB-order results for $\kappa=100,110,120,\ldots,200$, we obtain Fig. 12 [43]. We do not find exponential tails in this energy distribution, instead we observe simple power-law decay in the limits of small and large a.

A second important representation shows the energy-level contributions from

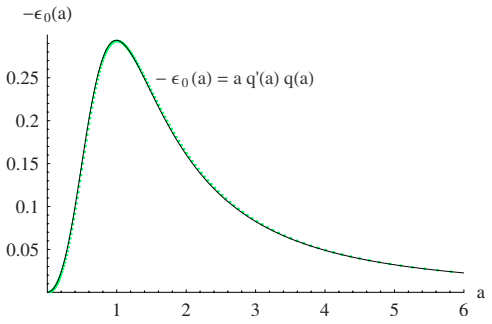

FIG. 12. (Color online) The (negative) energy density $-\epsilon_0(a)$ of the ground-state energy $E_0=\int_0^\infty da\epsilon_0(a)$, obtained from our analytical model function $q(a)$ as $-\epsilon(a)=aq'(a)q(a)$ (black curve), is shown to agree well with discrete numerical 200-RSB results (green dots).

$$\epsilon_0(l,\kappa) = -\frac{1}{4}\lim_{T\to 0} a_l(\kappa)[q_l^2(\kappa) - q_{l+1}^2(\kappa)], \tag{31}$$

as a function of normalized level index l/κ, and with boundary conditions $a_0=\beta$, $q_0=1$. The sum over all energy levels $\epsilon_0(l,\kappa)$ with level index $l=0,1,2,\ldots,\kappa$ for each calculated RSB order yields the RSB flow of the ground-state energy

$$E_0(\kappa) = \sum_{l=0}^{\kappa} \epsilon_0(l,\kappa) \tag{32}$$

towards the exact value [33] $E_0(\kappa=\infty)=E_0$. A proper normalization of level numbers by the RSB order κ, displays the level distributions for each RSB order on the same interval of unit length. Subsequent rescaling of the energy level allows one to visualize the RSB flow towards one fixed-point energy distribution (which of course depends on the rescaling factor [44]). Figure 13 shows two choices [l and κ rescaling of $\epsilon_0(l,\kappa)$]—in both cases the convergence towards the fixed-point function is obvious.

Fixed points (under RSB flow) have been calculated in the same way as shown before for the order function. For example, fixing l/κ to a rational number m/n within the unit interval, one can see many of the leading fixed points in Fig. 13 following the RSB flow along vertical lines fixed by m/n. The piecewise dense set of calculated fixed points was obtained by an extrapolated Padé approximation for $n=2,\ldots,51$ with $m=1,\ldots,n-1$. These fixed points are shown in Fig. 13 together with their fit function, obtained here as an (8,8)-Padé series. The fixed points are piecewise dense with some gaps near "leading" fixed points (e.g., which become, however, closed as higher orders are evaluated). The fit function (interpolating between the dense regions) represents an approximation for the exact fixed-point energy distribution function $\epsilon_0^*(\zeta)$ with $l/\kappa\to\zeta$ in the ∞-RSB limit. The numerical integration of the approximated function $\rho_\epsilon^*(\zeta)$ [which corresponds to $\epsilon^*(a)$ of Eq. (30) transformed from $0\leqslant a\leqslant\infty$ onto the unit interval $0\leqslant\zeta\leqslant 1$] yields [45]

$$E_0^* \equiv E^*(T=0) = \int_0^1 d\zeta \rho_\epsilon^*(\zeta)|_{approx} \approx -0.763\ 14. \tag{33}$$

By reproducing the correct value [33] up to $O(10^{-5})$, this provides a good test of the fixed-point method. An alternative calculation, using Eq. (30) with a plugged-in fixed-point order function confirms the numerical value E_0^*. The inserted figure shows the magnitude of energy corrections per level l occurring from 200 RSB to the exact ∞-RSB energy per level (recall that l labels the Parisi boxes of the RSB order parameter).

Different power-law decays are observed in the small l/κ ($\mathcal{CP}1$) and in the $l/\kappa\approx 1$ range near ($\mathcal{CP}2$).

B. Equilibrium susceptibility per level

To conclude this section we extend the described method to the $\chi(a)$ density of the equilibrium susceptibility χ and, in particular, to the distribution per level l. In the RSB limit, the total χ is known to be equal to 1 in the entire ordered phase. The RSB flow thus moves towards a fixed-point function $\chi(a)=aq'(a)$ with the property $\int_0^\infty da\chi(a)=1$ (this had been used before as a constraint for our analytical order function model [22,30]).

Let us now study the RSB flow of the discrete representation $\chi(l,\kappa)=a_l(\kappa)[q_l(\kappa)-q_{l+1}(\kappa)]$. The result for the susceptibility per level l (normalized by RSB order κ) is shown in Fig. 14 (and corresponds to the energy-per-level distribution shown in the preceding figure).

Beyond the flow of the finite RSB orders $\kappa=10,20,30,\ldots,200$ we have added the fixed-point function

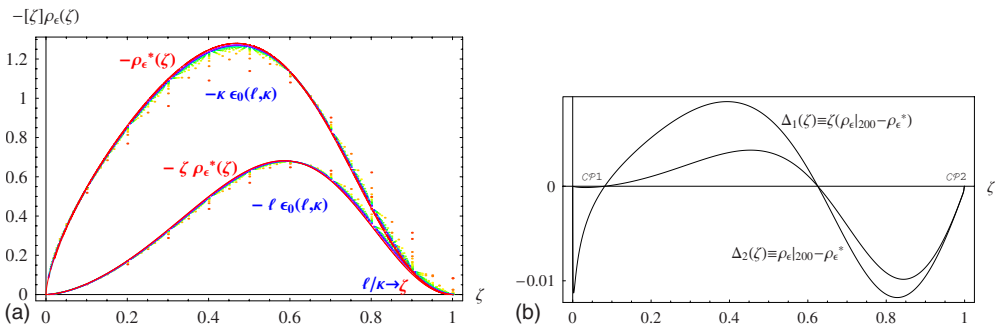

FIG. 13. (Color online) Part (a) shows ground-state energy solutions (dots) for $\kappa\epsilon_0(l,\kappa)$ [or $l\epsilon_0(l,\kappa)$] and their RSB flow from $\kappa=10$ to $\kappa=200$, $\Delta\kappa=10$, towards their fixed-point functions $[\zeta]\rho_\epsilon^*(\zeta)$ on the unit interval of levels $l/\kappa\to\zeta$. (b) shows differences $\Delta_{1,2}$ between 200 RSB (interpolation functions $[\zeta]\,\rho_\epsilon|_{200}$) and the fixed-point functions $[\zeta]\rho_\epsilon^*(\zeta)$ [red curves in (a)].

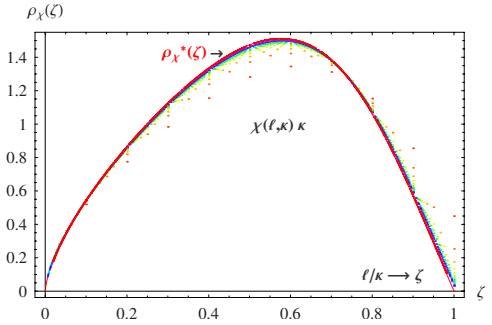

FIG. 14. (Color online) RSB flow of the equilibrium susceptibility per level l from $\kappa=10$ to $\kappa=200$ (in steps of ten orders of RSB and rescaled by $l\rightarrow l/\kappa$ to a unit interval) towards the fixed-point susceptibility distribution $\rho_\chi^*(\zeta)$ (red line).

$\rho_\chi^*(\zeta)$ for the susceptibility density [i.e., $\chi(a)$ transformed onto the unit interval $0\leqslant\zeta\leqslant 1$], which must obey $\int_0^1 d\zeta\rho_\chi^*(\zeta)=1$. A simple approximate calculation of the interpolating fixed-point function reproduces the exact constraint with an error of only $O(10^{-5})$. Again this confirms the power of the method, which can, e.g., be used to test analytical proposals.

Small changes from 200 RSB to ∞ RSB are resolved in Figs. 14 and 13. Their tendency is to make the distribution more symmetric. Yet the distribution per normalized level remains asymmetric as for the energy distribution (as a function of the dense levels l/κ), a universal fact that has been observed as a special feature of the SK model in contrast to symmetrical distributions finite-range spin glasses.

VIII. SCALING WITH THE PSEUDODYNAMICAL VARIABLE OF THE ORDER FUNCTION $q(a)$

In previous publications we found a Langevin-type representation [22,36] for a logarithmic derivative of the order function $q(a)$ with respect to $1/a$. This ordinary differential equation (without stochastic field) is much simpler than the exact partial differential equations, which is a consequence of the existence of scaling behavior and of homogeneous functions. It is well known that scale invariance and the so-called similarity method reduce partial to ordinary differential equations [46]. Therefore, at least near the critical points one can expect ordinary differential equations to describe RSB.

The Langevin type of differential equation could, however, be reshaped in terms of different pseudodynamic variable a, $1/a$, or other forms. The differential equation remains to be relaxational and thus there remains some arbitrariness in the choice of the proper "time" variable τ. If we wish to apply dynamic scaling to the RSB representation, we are unfortunately bound to make a definite choice. Let us consider $a+1/a$ as a pseudotime in order to conform with the expectation that critical behavior at either of the points $\mathcal{CP}1$ or $\mathcal{CP}2$ should occur in the long-time limit. Then at $\mathcal{CP}1$ we would get $\tau\sim a\rightarrow\infty$ while $\tau\sim\frac{1}{a}\rightarrow\infty$ at $\mathcal{CP}2$.

We may now consider pseudodynamical scaling by studying the a-dependent quantities like the order function near $\mathcal{CP}1$ and $\mathcal{CP}2$.

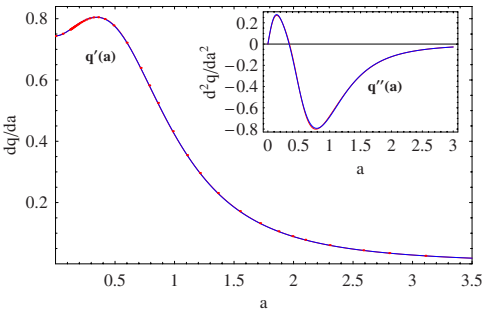

FIG. 15. (Color online) The characteristic maximum in $q'(a)$ is analytically well reproduced. Red dots show the discretized derivative obtained from 50 fixed point $\{a^*,q^*\}$. The inset shows the second derivative of the model order function $q(a)$.

Near $\mathcal{CP}1$ the order function obeys

$$q(a,\kappa,T)=1+a^{-2}f_q(T^2/a^{-2},a^2/\kappa^{10/3}), \tag{34}$$

with $f_q(x,0)\sim x$, $f_q(0,x)\sim x$, and $f_q(0,0)$ finite.

In terms of the transformed order function

$$\phi\sim\partial_{1/a}\ln(q(a)), \tag{35}$$

one gets $\phi\sim 1/a$ at $\kappa=\infty$, $T=0$ and $\phi\sim T$ at $a=\infty$, $\kappa=\infty$. If one defines an exponent β by $\phi\sim T^\beta$ (in analogy with standard phase transitions), one obtains $\beta=1$. Similarly, the characteristic RSB crossover "length" $\xi_\kappa\equiv\kappa_c\sim a^{3/5}\sim T^{-3/5}$ allows one to extract an exponent $\nu=3/5$, again by using the exponent definition $\xi\sim T^{-\nu}$ of standard critical phenomena. The analogy obviously uses a vanishing critical temperature $T_c=0$.

One would like to go one step further and identify a pseudodynamic exponent z according to the pseudo-time-length relation $\tau\sim\xi_\kappa^z$. However, this runs into the difficulty that a pseudotime $1/a$ would vanish near $\mathcal{CP}1$. As discussed, the choice $\tau=a+1/a$ allows one to describe both $\mathcal{CP}1$ and $\mathcal{CP}2$ as long-time limits, and the conclusion would be $z=5/3$ and $z\nu=1$. This set of exponents $\beta=1$, $\nu=3/5$, $z=5/3$ characterizes the universality class of RSB at $\mathcal{CP}1$ (for the given choice of variables). This should provide a hint for the desirable comparison with other systems, which may belong to a similar universality class (see also chapter outlook).

IX. DETAILED STRUCTURE OF THE ORDER FUNCTION DERIVATIVES $q'(a)$ AND $q''(a)$

The derivatives depend much more specifically on the pseudotime variable than $q(a)$ itself. Failure of an analytic model function becomes detectable more easily in the derivatives. In order to control our modeling, we studied analytical fits firstly of all 200-RSB data, and secondly of the 50 calculated fixed points. Taking $q'(a)$ directly from the analytical form $q(a)$ as given by Eq. (1), we find good agreement with the discretized slope calculated from the fixed points. This is demonstrated in the main part of Fig. 15. In addition, the insert shows the second derivative $\partial_a^2 q(a)$, where the two analytic models (red and blue curves) show a small difference. The maximum seen in $q'(a)$ expresses the Crisanti-Rizzo curvature [22,38], a slight nonlinearity of the

order function in the small-a regime. It is, however, this contribution, which renders an analytical fit rather awkward. An analytical model, which fits well the neighborhood of the critical points $a=0$ and $a=\infty$, can have a simpler shape [30], but we want to get the pseudodynamic crossover right as well. Global quantities such as the energy (integral over all a), picking up only relatively small contributions nearby the critical points, depend on the crossover regime modeling. This can be seen in Eq. (30) as well as in Fig. 12 for the energy density.

X. CONCLUSIONS

In this paper we formulated a scaling theory of the flow towards full replica symmetry breaking (RSB) at $T=0$, for finite temperatures, and for finite magnetic fields in the SK model. Several fixed-point functions of RSB flow were evaluated.

The analysis was guided by

(1) a large set of high-precision numerical data, with up to 200 self-consistently solved orders of replica symmetry breaking for the $T=0$ SK spin glass and still a high number of orders for finite temperatures and magnetic fields,

(2) the identification of two critical points (at zero temperature and zero magnetic field), which are distinguished by two different pseudodynamic limits as obtained in an analytic picture of a Langevin-type equation in Refs. [22,30], and

(3) representing nonanalytic behavior near each of these critical points in the framework of the scaling theory of critical phenomena.

Power laws and scaling functions were identified by fitting the leading 200-RSB orders of self-consistent solutions deep inside the SK spin-glass phase; noninteger exponents were found and identified as rational numbers, characteristic of one-dimensional RSB behavior. This one-dimensional (1D) character originates in correlations on the pseudolattice of RSB orders, as a function of the quasicontinuous variable $1/\kappa$. By means of scaling functions we demonstrated how this nonanalytic RSB behavior enters in temperature- and field-dependent power laws of the ordered phase.

The universality class of replica symmetry breaking in the SK model calls for comparison with other physical systems. Comparable features can, for example, be expected in the order parameter fixed-point function [47].

The decoupling of a magnetic-field-sensitive critical point from a temperature-sensitive one was embedded in an unconventional scaling hypothesis for the free energy and found to be consistent with the numerical data.

The RSB flow was used to generate an order parameter fixed-point function, serving as a crossover between the two different pseudodynamical critical limits. Its fine structure was revealed by the leading derivatives, again confirming the excellent agreement between analytical model and fixed-point function.

XI. OUTLOOK AND A SHORT DISCUSSION OF SIMILAR UNIVERSALITY CLASSES

The given description of RSB universal behavior in the SK model (SK-RSB) should stimulate the search for comparable behavior in different physical and interdisciplinary systems. Comparing the set of exponents given in this paper suggests a list of such candidates; for the sake of brevity we mention only a few.

The pseudodynamical differential equation for the low-temperature SK model as derived in Ref. [33] can be transformed into a Burgers-like equation with generalized coefficients [depending in general on $q'(a)$]. Its nonlinear part dominates at large a; the linear term dominates the small-a regime. Since random stirring is absent in this ∞-RSB flow equation, it differs from a one-dimensional Kardar-Parisi-Zhang (KPZ) equation also by a missing noise term [48,49]. A remarkable qualitative analogy, however, exists between the $a=0$ and the $a=\infty$ critical points of SK-RSB on one hand and linear (Edwards-Wilkinson) or nonlinear fixed points of the KPZ equation [48] on the other. In KPZ growth, the nonlinear part results from lateral correlation (parallel to the interface), while the nonlinear part of SK-RSB originates in the large-a regime with maximal order parameter $q(a)\to 1$. Recently, Canet and Moore [50,51] reported, apart from the exact 1D result for the dynamic exponent $z=\frac{3}{2}$, an approximate solution of RSB type for the KPZ equation, where the dynamic exponent assumed the value $z=(4+d)/3$ below two dimensions, hence $z=\frac{5}{3}$ in 1D, which can be made to agree with the pseudodynamic exponent of the RSB-SK model (under the conditions given in Sec. VIII).

However, critical exponents of different universality classes may coincide in special dimensions and do not provide final answers. Universal features can eventually be described by probability distributions with identical functional form. The numerical distributions given in Secs. VII and VIII should thus be studied further by analytical models. In pioneering work, Garel *et al.* studied energy distribution functions to scrutinize similarities and differences between spin glasses (SK and other) and directed polymers [52–56]. A relationship between directed polymers and the KPZ equation was described in Ref. [57]. Very remarkable is the fact that the 1D KPZ universality class is known to be connected with the Gaussian orthogonal ensemble (GOE) Tracy-Widom distribution [58,59]. Not only because of this analogy, it is important to search for a representation of the RSB-SK class within random matrix theory [60,61].

ACKNOWLEDGMENTS

We are indebted to Kay Wiese, Markus Müller, Thomas Garel, Andrea Crisanti, David Sherrington, Haye Hinrichsen, and Stefan Boettcher for stimulating discussions and helpful remarks. We thank Tommaso Rizzo for useful remarks and for sending recent work prior to publication [62]. We are indebted to Charles Gould and to Peter Reis for critical reading of our manuscript. We thank the DFG for partial and continued support of this research under Grant No. Op28/7-1.

[1] M. Mézard, G. Parisi, and M. A. Virasoro, *Spin Glass Theory and Beyond* (World Scientific, Singapore, 1987).

[2] A. P. Young, *Spin Glasses and Random Fields* (World Scientific, Singapore, 1998).

[3] G. Parisi, *Field Theory, Disorder and Simulations* (World Scientific, Singapore, 1992).

[4] S. Galam, Y. Gefen, and Y. Shapir, J. Math. Sociol. **9**, 1 (1982).

[5] S. Galam, J. Math. Psychol. **30**, 426 (1986), and references therein.

[6] P. G. Higgs, Phys. Rev. Lett. **76**, 704 (1996).

[7] F. David and K. J. Wiese, Phys. Rev. Lett. **98**, 128102 (2007).

[8] M. Lässig and K. J. Wiese, Phys. Rev. Lett. **96**, 228101 (2006).

[9] H. Orland and A. Zee, Nucl. Phys. B: Field Theory Stat. Syst. **620[FS]**, 456 (2002).

[10] A. Crisanti, L. Leuzzi, and G. Parisi, J. Phys. A **35**, 481 (2002).

[11] O. C. Martin, R. Monasson, and R. Zecchina, Theor. Comput. Sci. **265**, 3 (2001).

[12] D. Sherrington and S. Kirkpatrick, Phys. Rev. Lett. **35**, 1972 (1975).

[13] E. Marinari, A. Pagnani, and F. Ricci-Tersenghi, Phys. Rev. E **65**, 041919 (2002).

[14] M. Müller, Phys. Rev. E **67**, 021914 (2003).

[15] G. Parisi, J. Phys. A **13**, L115 (1980).

[16] G. Parisi, Phys. Rev. Lett. **50**, 1946 (1983).

[17] M. Talagrand, Ann. Math. **163**, 221 (2006); *Spin Glasses: A Challenge for Mathematicians—Cavity and Mean Field Models* (Springer-Verlag, Barlin, 2003).

[18] K. Binder and A. P. Young, Rev. Mod. Phys. **58**, 801 (1986).

[19] S. Boettcher, Eur. Phys. J. B **46**, 501 (2005).

[20] J.-P. Bouchaud, F. Krzakala, and O. C. Martin, Phys. Rev. B **68**, 224404 (2003).

[21] T. Aspelmeier, A. Billoire, E. Marinari, and M. Moore, J. Phys. A: Math. Theor. **41**, 324008 (2008).

[22] R. Oppermann, M. J. Schmidt, and D. Sherrington, Phys. Rev. Lett. **98**, 127201 (2007).

[23] In addition to $1/\kappa$ we also consider scaling with respect to the pseudodynamic variable $1/a$, treating both as quasicontinuous scaling variables—one may imagine the analogy of a large enough lattice in real space, such that the discreteness of momenta can be neglected.

[24] M. E. Fisher, Rev. Mod. Phys. **46**, 597 (1974).

[25] P. Le Doussal, M. Müller, and K. J. Wiese, Phys. Rev. B **77**, 064203 (2008).

[26] D. S. Fisher and H. Sompolinsky, Phys. Rev. Lett. **54**, 1063 (1985).

[27] D. S. Fisher and D. A. Huse, Phys. Rev. B **38**, 373 (1988); **38**, 386 (1988); Phys. Rev. Lett. **56**, 1601 (1986).

[28] C. De Dominicis, I. Giardina, E. Marinari, O. C. Martin, and F. Zuliani, Phys. Rev. B **72**, 014443 (2005).

[29] C. Monthus and T. Garel, J. Phys. A: Math. Theor. **41**, 115002 (2008).

[30] R. Oppermann and D. Sherrington, Phys. Rev. Lett. **95**, 197203 (2005).

[31] S. Pankov, Phys. Rev. Lett. **96**, 197204 (2006).

[32] M. Müller and S. Pankov, Phys. Rev. B **75**, 144201 (2007).

[33] M. J. Schmidt and R. Oppermann, Phys. Rev. E **77**, 061104 (2008).

[34] G. Parisi and G. Toulouse, J. Phys. (Paris), Lett. **41**, L361 (1980).

[35] H. Sompolinsky, Phys. Rev. Lett. **47**, 935 (1981).

[36] R. Oppermann and M. J. Schmidt, Phys. Status Solidi C **4**, 3347 (2007).

[37] M. Ha, J. Timonen, and M. den Nijs, Phys. Rev. E **68**, 056122 (2003).

[38] A. Crisanti and T. Rizzo, Phys. Rev. E **65**, 046137 (2002).

[39] Recalling that H is not the conjugate field of the order parameter.

[40] We thank Thomas Garel for drawing our attention to the paper by Bouchaud *et al.* [20].

[41] T. Garel (private communication).

[42] D. Sherrington (private communication).

[43] On the given scale, all numerical results fall almost exactly onto the single analytical curve for $\epsilon_0(a)$; only extreme magnification reveals the RSB flow of the numerical data and tiny deviations from the analytical model in the crossover regime between $\mathcal{CP}1$ and $\mathcal{CP}2$.

[44] One may choose rescaling factors such that discrete spacing of energy levels would survive even in the fixed-point function $(\kappa=\infty)$ near $l/\kappa=0$ and $l/\kappa=1$; this would correspond to the discrete spectra of parameter ratios discussed in the paper.

[45] We tacitly assume here that the density functions $\rho_{\epsilon}^{*}(\zeta)$ and also $\rho_{\chi}^{*}(\zeta)$ (below) are Riemann integrable. The upgrade from the set of rational numbers l/κ to a continuous variable ζ could, in principle, hide a mathematically subtle problem, if the density functions were highly discontinuous and would, for example, require a Lebesgue integral.

[46] L. Debnath, *Nonlinear Partial Differential Equations* (Birkhäuser, Boston, 2004).

[47] A. A. Middleton, P. Le Doussal, and K. J. Wiese, Phys. Rev. Lett. **98**, 155701 (2007).

[48] A.-L. Barabási and H. E. Stanley, *Fractal Concepts in Surface Growth* (Cambridge University Press, Cambridge, 1995).

[49] M. Kardar, G. Parisi, and Yi-Cheng Zhang, Phys. Rev. Lett. **56**, 889 (1986).

[50] L. Canet and M. A. Moore, Phys. Rev. Lett. **98**, 200602 (2007).

[51] E. Bertin, Phys. Rev. Lett. **95**, 170601 (2005).

[52] C. Monthus and T. Garel, Phys. Rev. E **69**, 061112 (2004).

[53] C. Monthus and T. Garel, Phys. Rev. E **73**, 056106 (2006).

[54] M. Mézard and G. Parisi, J. Phys. I **1**, 809 (1991).

[55] C. Monthus and T. Garel, Phys. Rev. E **74**, 051109 (2006).

[56] T. Garel and H. Orland, Phys. Rev. B **55**, 226 (1997).

[57] M. Lässig, Nucl. Phys. B: Field Theory Stat. Syst. **448[FS]**, 559 (1995).

[58] P. L. Ferrari and H. Spohn, J. Phys. A **38**, L557 (2005).

[59] M. Prähofer and H. Spohn, Phys. Rev. Lett. **84**, 4882 (2000).

[60] K. Johansson, Commun. Math. Phys. **209**, 437 (2000).

[61] S. N. Majumdar, e-print arXiv:cond-mat/0701193.

[62] G. Parisi and T. Rizzo, e-print arXiv:0811.524